Original Article

Evaluation of various boluses in dose distribution for electron therapy of the chest wall with an inward defect

Hoda Mahdavi, Keyvan Jabbari[1], Mahnaz Roayaei

Department of Radiotherapy, Seyed al-Shohada Hospital, Isfahan University of Medical Sciences, [1]Department of Medical Physics and Engineering, School of Medicine, Isfahan University of Medical Sciences, Isfahan, Iran

Received on: 04-11-2015 **Review completed on:** 19-12-2015 **Accepted on:** 19-12-2015

ABSTRACT

Delivering radiotherapy to the postmastectomy chest wall can be achieved using matched electron fields. Surgical defects of the chest wall change the dose distribution of electrons. In this study, the improvement of dose homogeneity using simple, nonconformal techniques of thermoplastic bolus application on a defect is evaluated. The proposed phantom design improves the capability of film dosimetry for obtaining dose profiles of a patient's anatomical condition. A modeled electron field of a patient with a postmastectomy inward surgical defect was planned. High energy electrons were delivered to the phantom in various settings, including no bolus, a bolus that filled the inward defect (PB0), a uniform thickness bolus of 5 mm (PB1), and two 5 mm boluses (PB2). A reduction of mean doses at the base of the defect was observed by any bolus application. PB0 increased the dose at central parts of the defect, reduced hot areas at the base of steep edges, and reduced dose to the lung and heart. Thermoplastic boluses that compensate a defect (PB0) increased the homogeneity of dose in a fixed depth from the surface; adversely, PB2 increased the dose heterogeneity. This study shows that it is practical to investigate dose homogeneity profiles inside a target volume for various techniques of electron therapy.

Key words: Bolus, electron, mastectomy, radiotherapy

Introduction

Radiotherapy, following mastectomy, improves locoregional control as well as survival rates in breast cancer patients.[1-6] Photon tangential fields are commonly used for chest wall radiotherapy, but the choice of radiotherapy technique is not clearly demonstrated.[4] Patients with little tissue between their lung and skin are sometimes selected for electron therapy. Electrons are also used for patients who are unsuitable for photon therapy due to their anatomical characteristics, or in settings of reirradiation.[7-9] This can be performed by treating the entire chest wall with three or more abutting electron fields.[7] Electron therapy has comparable locoregional and survival benefits to those of photon techniques.[1,2,10,11]

Chest wall radiotherapy is often aided by tissue equivalent material termed bolus to bring isodose lines toward the surface. Dosimetric measurements of superficial regions of a phantom by a parallel plate chamber have shown that bolus is required to encompass superficial targets within the 90% isodose contour when treated by 6–22 MeV electrons.[12] Moreover, there is a risk of lung toxicity when using high energy electrons for chest wall radiotherapy.[13,14] In these cases, bolus can be used to protect deep structures.[15,16] Thermoplastic bolus can be finely conformed to the surface outline when heated and becomes rigid when cooled.[17]

Radiochromic films have a low energy dependence.[18] The electron stopping power of the sensitive material of radiochromic films is similar to water and muscle, and its

Address for correspondence:
Dr. Mahnaz Roayaei,
Department of Radiotherapy, Seyed al-Shohada Hospital,
Isfahan University of Medical Sciences, Isfahan, Iran.
E-mail: roayaei@med.mui.ac.ir

Access this article online	
Quick Response Code:	Website: www.jmp.org.in
	DOI: 10.4103/0971-6203.177288

How to cite this article: Mahdavi H, Jabbari K, Roayaei M. Evaluation of various boluses in dose distribution for electron therapy of the chest wall with an inward defect. J Med Phys 2016;41:38-44.

response to electron beam irradiation has an estimated uncertainty of within ±5% at 95% confidence level.[19] Radiochromic films have been used for measuring surface doses in electron therapy.[17]

The standard dose distribution of electrons is perturbated by structural and tissue variations.[20] Dosimetric hot and cold spots can cause acute and late adverse tissue reactions and reduce treatment effectiveness. Nonuniform thickness boluses have been used in electron conformal therapy (ECT) so that the distal edge of the target volume receives the minimum therapeutic dose.[21-24] The facilities needed for ECT are not vastly available. Nonconformal methods of electron therapy are simple and still practiced in many centers.

In this study, a phantom of a patient with a large defect on her chest wall is constructed based on her digital imaging and communications in medicine (DICOM) images from Perspex as tissue and composite cork as lung substitute.[25] A single electron field is treated accordingly. Gafchromic film dosimetry was used to obtain profiles across the defect.[26,27] The effect of thermoplastic bolus application on dose homogeneity in the target beneath the inward defect is assessed. Standard anthropomorphic phantoms have axial cuts that limit measurements to certain directions of the beam. The design of the phantom extends the capability of film dosimetry for assessing dose uniformity inside the phantom at a fixed distance from the source and a desired gantry angle.

Materials and Methods

Planning

A patient with right mastectomy and an inward defect at the lateral end of her mastectomy scar was selected. The inward defect was 2 cm wide with a steep edge at the supralateral side. It was located near the midportion of the anterior axillary line. A multislice computed tomography (CT) scan of the patient was taken in the treatment position. TIGRT treatment planning system (Linatech, China, Shanghai) was used to contour the chest wall clinical target volume (CTV) based on the radiation therapy oncology group reference atlas for high risk breast cancer, and to define the electron field borders with 1 cm margin to the defected volume (CTV1), and the gantry angle. Isodose curves and dose-volume histograms were not used for planning purposes. The original field was 11.5 cm × 11.5 cm, angled 311° and contained 30° of chest wall curvature.

Phantom and bolus design

DICOM data of CT images of the patient was imported in the 3D-doctor software (Able Software Corp, USA) to model the chest and right lung. To simplify the design, a rotation to the CT images was applied to make the incident beam perpendicular to the layers when the gantry is at angle 0. Borders of the lung parenchyma and chest were defined by interactive segmentation which was available in this software. Rib cage, lung hilum structures, as well as the bronchi segments, were not included in this model. The three-dimensional (3D) model of the lung and the chest were then virtually resliced along a plane perpendicular to the beam to create layers with desired thickness. The 2D contours of the lung and chest layers were inputted to the laser cutter software.

Clear Perspex was used as a substitute for chest. The measured density of Perspex was 1.04 g/cm^3. Layers of 5 mm were used for the first 3 cm of the chest wall and 10 mm for the rest. Sheets of composite cork were used for the lung substitute. The cork sheets were 5 mm thick, and the measured density was 0.2 g/cm^3. Thermoplastic bolus sheets and pellets (Orfit, Wijnegem, Belgium) were used on the phantom surface to create a bolus that filled the inward defect (PB0), and uniform layers of 5 mm (PB1) and 2 layers of 5 mm bolus were used for creating PB2. The pellet bolus made the maximum thickness of 50 mm from the defect to the flat surface. The defect is shown in Figure 1. The CT Hounsfield unit of standard cork was in the range of −900 to −600 HU, and this value was −10–200 HU for both the Perspex and bolus. Figure 2 shows CT sections of the phantom with bolus.

Energy selection

The energy of the beam was selected so that the isodose level at the chest wall-lung interface was approximately 80% to spare the lung.[18] This selection was done from the available energies, and percentage depth dose charts of the Oncor (Siemens Healthcare, Erlangen, Germany) linear accelerator. Electron energies of 12 MeV and 15 MeV were used. While for the 12 MeV beam the 80% and 90% isodose lines occurred at the depths of 4.5 cm and 4 cm respectively, for the 15 MeV the same occurred at the depths of 5.5 cm and 5 cm. D_{max} is 29 mm for E12 and 32 mm for E15 in the central axis in a standard water phantom.

Dosimetry

Small films of Gafchromic® EBT2 (Ashland Specialty Ingredients, NJ, USA) were placed horizontally in-between the phantom Perspex layers within the CTV1. This type of film is not very sensitive to visible light, and, therefore, it can easily be cut without needing a dark room. The orientation was chosen to record most of the varying depth. The films were placed in a supralateral to inframedial direction, so the effect of chest wall curvature was negligible. The orientation and alignment of the films were inked. Dosimetric regions of interest were 3 cm × 13 cm profiles across the defect. Three profiles were assessed in this study that were placed at the deepest surface of the defect (layer 0), 10 mm deeper (layer 10), and 20 mm deeper (layer 20) from the first film. Films were also placed at the surface of the lung and similar points along the depth of the lung with intervals of 1 cm, and the surface of the right heart.

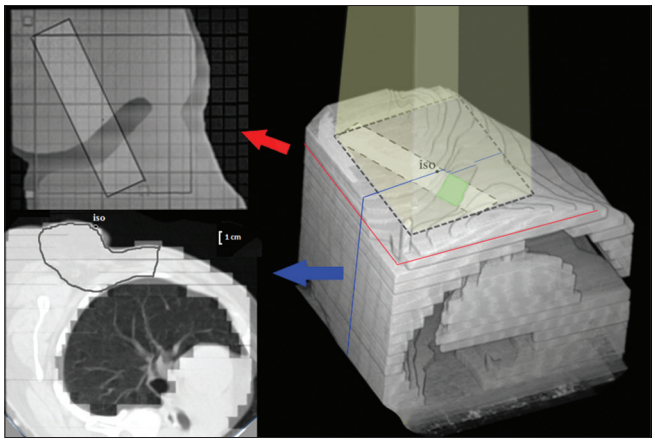

Figure 1: Right: Three-dimensional volume reconstructions of the computed tomography images of the phantom. The rectangle shows the position of the Gafchromic film in XY dimension and the square shows the electron field. Left: Axial and coronal cuts from the phantom. The coronal cut crosses the film at layer 0. The axial cut crosses the isocenter. A fusion of the phantom and the computed tomography image of the patient is shown in the axial cut, and the original clinical target volume 1 is contoured

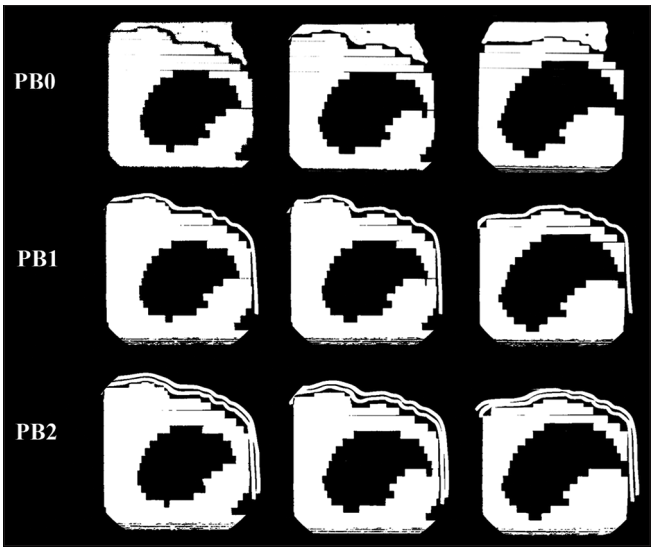

Figure 2: Different computed tomography sections of the phantom with bolus. PB0: Pellet bolus filling the defect, PB1: 5 mm bolus, PB2: Two 5 mm bolus

Setup and radiation

The source to surface distance (SSD = 100 cm) was set at the surface of the phantom. The SSD was not set at the surface of the bolus when bolus was inserted. The prescribed dose was 200 cGy (200 monitor units in all experiments) to D_{max} with electrons 12 MeV and 15 MeV with no bolus (NB), or boluses PB0, PB1, and PB2.

Dose reading

A 9800 scanner XL (Microtech CO., Hsinchu, Taiwan) was used for scanning film series. The resolution of the scanner was set to 300 dots per inch. A central area of 20 mm × 90 mm (of the 30 mm × 13 mm films) was chosen for dose reading to minimize the effect of dose gradients and dosimetric artifacts. The red channel of the image was selected for measurements.[26]

For the lung point of interest (POI) doses, the mean dose of an area of 30 × 30 pixels at the center of each film was read to reduce the possibility of the effect of artifacts. Using an in-house code in MATLAB software (MathWorks, MA, USA), doses were read and measured by calculating the optical density. The means and standard deviations (SD) of each profile were recorded. Relative SD (RSD) was used as an indicator for dose inhomogeneity.

Results

Profiles

As demonstrated in Table 1, bolus application reduced the mean dose at each profile when compared to NB. The mean dose was higher with PB0 than other types of bolus in layers 0 and 10. Results showed a more desirable dose homogeneity with pellet bolus that filled the defect completely (PB0), compared to PB1 or PB2. The profiles were more uniform in dose homogeneity for 15 MeV than 12 MeV for both surface and depth of CTV1. Figure 3 illustrates selected 2D dose profiles. High dose regions at the edges of the defect can be seen at level 0 when NB was applied and was not seen when bolus was used. Dose ratio had the maximum value of 111.5% in this area for 12 MeV electrons and 108.5% for 15 MeV electrons. The hot area was also evident at the profiles located 10 mm below the defect. The dose ratio of the hot area was even higher at this level (113.5% for 12 MeV and 112.5% for 15 MeV).

Table 1: Mean dose (cGy) and standard deviation of profiles at the deepest part of the defect (layer 0), and 1 cm below (layer 10), and 2 cm below the level of the defect (layer 20) for each experiment

Profile	*12 MeV*			*15 MeV*		
	M	*SD*	*RSD (%)*	*M*	*SD*	*RSD (%)*
Layer 0						
NB	192.0	12.8	6.7	189.6	10.1	5.3
PB0	193.1	9.8	5.1	180.2	6.4	3.6
PB1	154.3	9.8	6.4	156.2	6.6	4.2
PB2	145.4	18.8	12.9	153.0	7.9	5.2
Layer 10						
NB	168.3	18.1	10.8	181.5	10.3	5.7
PB0	143.9	14.6	10.1	165.9	7.1	4.2
PB1	113.9	29.6	26.0	134.0	15.9	11.9
PB2	94.1	48.1	51.1	125.5	21.3	17.0
Layer 20						
NB	119.1	50.1	42.1	159.6	25.4	15.9
PB0	56.9	17.4	30.6	125.7	14.8	11.8
PB1	60.8	51.6	84.9	106.8	31.7	29.7
PB2	44.0	49.0	111.4	86.4	40.1	46.4

M: Mean dose, SD: Standard deviation, RSD: Relative standard deviation, PB0: Pellet bolus filling the defect, PB1: 5 mm bolus layer, PB2: Two 5 mm bolus layers, NB: No bolus

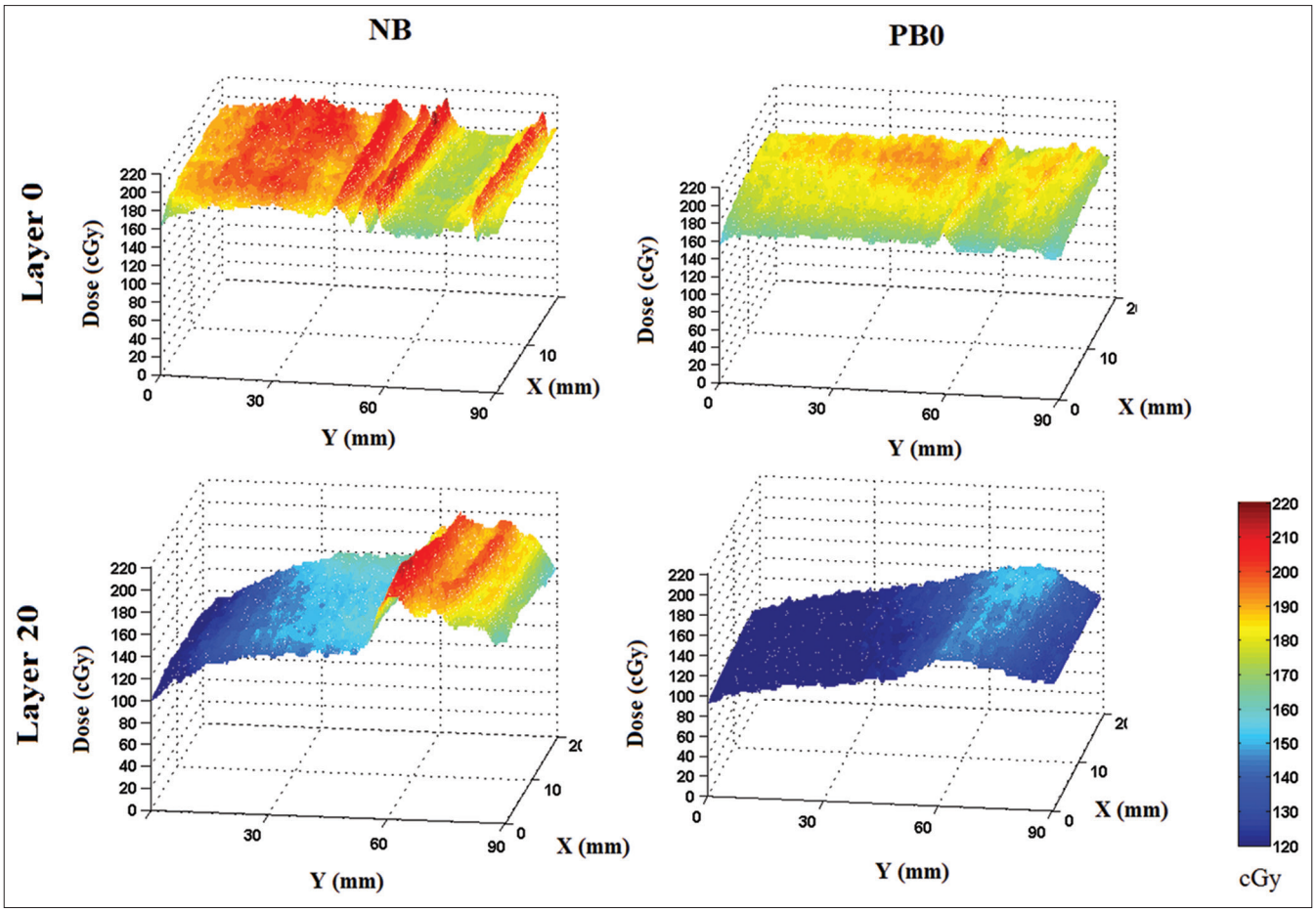

Figure 3: Sample two-dimensional profiles of the dose across the defect measured with film dosimetry of films located at the deepest part of the defect (layer 0), and 2 cm below the defect (layer 20) for 15 MeV electrons. NB: No bolus, PB0: Pellet bolus filling the defect

No hot areas were observed in profiles at 20 mm below the defect.

Lung

Table 2 shows the measured doses inside the lung that started from the chest wall pleural interface (POI 1) and increments of 1 cm deeper. The bolus reduced the dose to the lung POIs. The amount of dose reduction with PB0 was greater and seemed more uniform in different depths compared to PB1 and PB2 that reduced the dose of deeper POIs to a greater amount [Table 2].

Heart

The dose received at the surface of the modeled right ventricle was on a plane perpendicular to the electron beam at the distance of 7 cm from the lung surface and outside the primary field. The measured dose profile at this level showed that the highest dose of each experiment was delivered to the inframedial portion of the heart that was the surface of the muscular right ventricle. The measured dose was lowest when it was irradiated with 15 MeV electrons, and the PB0 was used (4.6 cGy), and with 12 MeV electrons and the PB2 (4.7 cGy), and highest when irradiated with 12 MeV electrons without bolus (54.3 cGy), and 15 MeV electrons without bolus (51.4 cGy).

Table 2: The depth doses read from the Gafchromic films for 12 MeV and 15 MeV electrons inside the lung and the percent of dose reduction compared with no bolus showed in brackets. Depth is measured from the deepest surface of the defect

E	*POI*	*NB*	*PB1*	*PB2*	*PB0*
12 MeV	1	205.3	134.7 (34.3)	124.7 (39.3)	67.2 (67.3)
	2	149.7	102.3 (31.6)	95.7 (36.7)	43.2 (71.1)
	3	166.7	106.0 (36.4)	64.7 (61.2)	28.9 (82.7)
	4	137.6	84.5 (38.6)	48.6 (64.7)	29.8 (78.3)
15 MeV	1	166.5	150.4 (9.7)	122.3 (26.5)	93.5 (43.8)
	2	186.6	138.1 (26)	128.4 (31.2)	119 (36.2)
	3	183.6	144.2 (27.3)	143.2 (22)	145.5 (20.7)
	4	137.7	51.9 (62.3)	70.6 (48.7)	85.5 (37.9)

POI 1: At the chest-wall pleural interface, POI 2: At 1 cm depth, POI 3: At 2 cm depth, POI 4: At 3 cm depth, PB0: Pellet bolus filling the defect, PB1: 5 mm bolus, PB2: Two 5 mm bolus, NB: No bolus, E: Electron beam energy

Discussion

The findings of this study showed that in electron therapy of a chest wall with a defected surface, bolus can decrease the mean dose to the base of the defect by reducing dose heterogeneity and eliminating areas that receive doses

higher than D_{max}. Whereas application of bolus is usually intended for increasing the dose to the surface. At a flat surface, the dose delivered by high energy electrons is at least 85% of the D_{max}, and this can approach D_{max} with bolus. Dose reduction should be carefully considered when the CTV is at close approximation with an irregular surface.[18]

Dose homogeneity

The Dose profile was more homogenous when using the pellet bolus that completely filled the defect (PB0) compared to all other boluses. Dose variation increased when 12 MeV electrons were used with the PB2 compared with NB. The relative SD in this condition was the highest value, indicating that bolus should be used with caution when the purpose is to reduce dose heterogeneity.

The electron energy estimation for the dose coverage of the CTV1 was suboptimal by conventional electron therapy planning. The deepest border of the CTV1 received 80 cGy for 15 MeV and NB while an adequate surface dose and a dose coverage of at least 80% at the deep border was expected. It can be seen in Figure 3 that at the location of the defect at layer 0, the dose is less than adjacent areas without a bolus. This result can be explained by the loss of side scatter equilibrium and inadequate build-up at defected surfaces. Irregular surfaces cause local scattering. Moreover, steep surface depressions cause electrons to scatter inwardly.[27] These effects cause difficulties in predicting the desired beam energy based on axial images. It should be taken into account that bolus material, in practice, did not fit to all steps of the phantom surface, and long air-gaps were seen in CT sections. Air-gaps can contribute to the low doses at layer 0 when either bolus was applied. These air-gaps change the electron fluence and reduce the surface dose, especially in lower energy electrons and larger field sizes.[28,29] Similar gaps can be created in a real clinical setting depending on the amount of obedience of the moldable bolus from the surface topology. Rigid bolus may reduce trivial soft tissue irregularities of the surface, and therefore, reduce air-gaps,[30] but the additive effect of variable day-to-day bolus placement, and soft tissue changes during treatment may also be considerable when a rigid bolus is used.

The dose profiles showed that the dose reduced underneath the stepped surface and hot areas near the base of the steep edge were created. The observed hot areas at the surface of the phantom were compatible with the effect of stepped edges that causes side scatter disequilibrium.[7,27] No hot areas were observed in the layers when bolus was used. This means less acute and late soft tissue complications are expected when the bolus is used in a similar clinical case.

This study suggests that because of depth dose uncertainty of conventional (nonconformal) electron therapy with bolus application, this may not be a good option in a defected chest wall, particularly when deep structures such as the lower axillary levels are supposed to be targeted. In bolus ECT, however, data from tissue inhomogeneity and the topology of the target volume are all integrated for bolus design, yet, limitations of achieving dose homogeneity,[31] air-gaps, and other setup uncertainties remain when custom boluses are designed for desirable dose coverage. Therefore, well-commissioned planning system that can handle custom bolus beside *in vivo* dosimetry verification is worthy and is recommended for chest wall electron therapy.[19]

Lung

The presence of boluses resulted in reduced lung doses which was along expected lines. The expected depth dose decreasing pattern of POIs by depth was not seen in doses read from the films. In fact, when 15 MeV electron was used for the phantom, the measured dose values were lower at 1 cm depth than a corresponding point at 2 cm beneath the chest wall-lung interface. The dose at this point did not seem to be substantially affected by the thickness of the overlying bolus [Table 2]. This can be explained by the dose gradients caused by anatomic and tissue heterogeneities. The coefficient of equivalent thickness (CET) of the lung is variable with depth. This phenomenon may also explain the dose increase at some distance from the lung surface. A scatter reduction occurs as electrons enter the low-density lung, but as the electrons proceed, the increased penetration overtakes the reduced scatter and dose starts to increase.[26]

The dose values showed the fact that the electron beam penetration is higher in cork than in Perspex. This was more prominent for the higher energy electrons. This is compatible with physics of electron therapy.[17] The 40% isodose contour that represents a threshold for pneumonitis in breast radiotherapy may be three to 4 times further in the lung than soft tissue.[30] Radiation injury to the lung has been detected in more than a third of patients treated with electrons and has been related to dosimetric and patient factors.[15] The convex surface of the lung causes manual calculation of depth doses based on the CET difficult. It can be concluded that selection of the energy of the electron based on PDD charts and thickness of the tissue may not be appropriate in a similar setting.

Heart

The measured doses in the phantom showed that in this clinical case, the proximal surface of the heart could receive up to 1357 cGy if 12 MeV is used for the patient with NB from this single field throughout the entire treatment regimen by conventional doses of standard fractionation (i.e. 50Gy). This dose value would have reduced to 227 cGy if PB0 was applied. Adding other fields would increase the received dose. An increased risk of ischemic heart disease is not expected in postmastectomy patients who are treated with electrons.[32] However, in instances where the thickness of target volume of the chest is variable, the integral dose underlying the thinnest portion (e.g., a defect) will be

higher.[33] when higher electron energies and bolus are used for dose conformity, the dose to the heart can be more significant.

Some of the limitations of this study are first the problem of the change of the SSD when the bolus was placed. This can cause some errors in comparing each setting. The available data from the machine showed that when the SSD changes from 100 cm to 99 cm, the output of the machine will have a small increase to approximately 2%. This should be taken into account when comparing the results for each bolus placement. Second, the limitation of carving the chest wall defect caused stepped layers and consequent dosimetric errors. This can be improved with 3D cutters in future work.

Conclusion

The current study showed that in a 2D, nonconformal electron therapy plan of the chest wall, a bolus that compensates an inward defect can improve dose profile homogeneity of the CTV. This effect is provided by increasing dose to the base and reducing high dose regions at steep edges of the defect. Dose homogeneity is desirable for reducing acute and late tissue injury when dose coverage to the distal target volume is assured.

If a bolus is used, the treatment effectiveness is affected by the time-consuming preparation, different day-to-day set up, air gaps, and *in vivo* dose verification.

Acknowledgments

The authors would like to thank Dr. Alireza Amouheidari, the head of radiotherapy department of Isfahan Milad hospital, who kindly provided us with facilities and useful comments. We also thank to Shahram Monadi for comments in experimental design of the study.

Financial support and sponsorship

This study was supported in part by a research grant from Isfahan University of Medical Sciences.

Conflicts of interest

There are no conflicts of interest.

References

1. Overgaard M, Hansen PS, Overgaard J, Rose C, Andersson M, Bach F, *et al.* Postoperative radiotherapy in high-risk premenopausal women with breast cancer who receive adjuvant chemotherapy. Danish Breast Cancer Cooperative Group 82b Trial. N Engl J Med 1997;337:949-55.
2. Overgaard M, Jensen MB, Overgaard J, Hansen PS, Rose C, Andersson M, *et al.* Postoperative radiotherapy in high-risk postmenopausal breast-cancer patients given adjuvant tamoxifen: Danish Breast Cancer Cooperative Group DBCG 82c randomised trial. Lancet 1999;353:1641-8.
3. Ragaz J, Olivotto IA, Spinelli JJ, Phillips N, Jackson SM, Wilson KS, *et al.* Locoregional radiation therapy in patients with high-risk breast cancer receiving adjuvant chemotherapy: 20-year results of the British Columbia randomized trial. J Natl Cancer Inst 2005;97:116-26.
4. Recht A, Edge SB, Solin LJ, Robinson DS, Estabrook A, Fine RE, *et al.* Postmastectomy radiotherapy: Clinical practice guidelines of the American Society of Clinical Oncology. J Clin Oncol 2001;19:1539-69.
5. Rutqvist LE, Rose C, Cavallin-Ståhl E. A systematic overview of radiation therapy effects in breast cancer. Acta Oncol 2003;42:532-45.
6. Whelan TJ, Julian J, Wright J, Jadad AR, Levine ML. Does locoregional radiation therapy improve survival in breast cancer? A meta-analysis. J Clin Oncol 2000;18:1220-9.
7. Buchholz TA, Wazer DE, Haffty BG. Breast cancer: Locally advanced and recurrent disease, postmastectomy radiation, systemic therapies. In: Halperin EC, Brady LW, Wazer DE, Perez CA, editors. Perez & Brady's Principles and Practice of Radiation Oncology. 6th ed. Philadelphia: Lippincott Williams & Wilkins; 2013. p. 1160-2.
8. Perkins GH, McNeese MD, Antolak JA, Buchholz TA, Strom EA, Hogstrom KR. A custom three-dimensional electron bolus technique for optimization of postmastectomy irradiation. Int J Radiat Oncol Biol Phys 2001;51:1142-51.
9. Kudchadker RJ, Hogstrom KR, Garden AS, McNeese MD, Boyd RA, Antolak JA. Electron conformal radiotherapy using bolus and intensity modulation. Int J Radiat Oncol Biol Phys 2002;53:1023-37.
10. Feigenberg SJ, Price Mendenhall N, Benda RK, Morris CG. Postmastectomy radiotherapy: Patterns of recurrence and long-term disease control using electrons. Int J Radiat Oncol Biol Phys 2003;56:716-25.
11. Gez E, Assaf N, Bar-Deroma R, Rosenblatt E, Kuten A. Postmastectomy electron-beam chest-wall irradiation in women with breast cancer. Int J Radiat Oncol Biol Phys 2004;60:1190-4.
12. Gerbi BJ. The response characteristics of a newly designed plane-parallel ionization chamber in high-energy photon and electron beams. Med Phys 1993;20:1411-5.
13. Pierce LJ, Wazer DE, Vora SR. Radiation therapy techniques for newly diagnosed non-metastatic breast cancer. In: Uptodate, Post TW (Ed), UpToDate, Waltham, MA. Available from: http://www.uptodate.com/contents/radiation-therapy-techniques-for-newly-diagnosed-non-metastatic-breast-cancer. [last accessed on 2015 Oct 10].
14. Wennberg B, Gagliardi G, Sundbom L, Svane G, Lind P. Early response of lung in breast cancer irradiation: Radiologic density changes measured by CT and symptomatic radiation pneumonitis. Int J Radiat Oncol Biol Phys 2002;52:1196-206.
15. Huang EY, Wang CJ, Chen HC, Sun LM, Fang FM, Yeh SA, *et al.* Multivariate analysis of pulmonary fibrosis after electron beam irradiation for postmastectomy chest wall and regional lymphatics: Evidence for non-dosimetric factors. Radiother Oncol 2000;57:91-6.
16. Kirova YM, Campana F, Fournier-Bidoz N, Stilhart A, Dendale R, Bollet MA, *et al.* Postmastectomy electron beam chest wall irradiation in women with breast cancer: A clinical step toward conformal electron therapy. Int J Radiat Oncol Biol Phys 2007;69:1139-44.
17. Khan FM, Gibbons JP. Electron beam therapy. In: Khan FM, Gibbons JP, editors. Khan's the Physics of Radiation Therapy. 5th ed. Philadelphia: Lippincott Williams & Wilkins; 2013. p. 256-308.
18. Niroomand-Rad A, Blackwell CR, Coursey BM, Gall KP, Galvin JM, McLaughlin WL, *et al.* Radiochromic film dosimetry: Recommendations of AAPM Radiation Therapy Committee Task Group 55. American Association of Physicists in Medicine. Med Phys 1998;25:2093-115.
19. Gerbi BJ, Antolak JA, Deibel FC, Followill DS, Herman MG, Higgins PD, *et al.* Recommendations for clinical electron beam dosimetry: Supplement to the recommendations of Task Group 25. Med Phys 2009;36:3239-79.
20. Boone ML, Almond PR, Wright AE. High-energy electron dose perturbations in regions of tissue heterogeneity. Ann N Y Acad Sci

1969;161:214-32.
21. Olofsson L, Mu X, Nill S, Oelfke U, Zackrisson B, Karlsson M. Intensity modulated radiation therapy with electrons using algorithm based energy/range selection methods. Radiother Oncol 2004;73:223-31.
22. Opp D, Forster K, Li W, Zhang G, Harris EE. Evaluation of bolus electron conformal therapy compared with conventional techniques for the treatment of left chest wall postmastectomy in patients with breast cancer. Med Dosim 2013;38:448-53.
23. van der Laan HP, Korevaar EW, Dolsma WV, Maduro JH, Langendijk JA. Minimising contralateral breast dose in post-mastectomy intensity-modulated radiotherapy by incorporating conformal electron irradiation. Radiother Oncol 2010;94:235-40.
24. Gauer T, Engel K, Kiesel A, Albers D, Rades D. Comparison of electron IMRT to helical photon IMRT and conventional photon irradiation for treatment of breast and chest wall tumours. Radiother Oncol 2010;94:313-8.
25. Chang KP, Hung SH, Chie YH, Shiau AC, Huang RJ. A comparison of physical and dosimetric properties of lung substitute materials. Med Phys 2012;39:2013-20.
26. Jabbari K, Rostampour M, Roayaei M. Monte Carlo simulation and film dosimetry for electron therapy in vicinity of a titanium mesh. J Appl Clin Med Phys 2014;15:4649.
27. Devic S, Seuntjens J, Sham E, Podgorsak EB, Schmidtlein CR, Kirov AS, *et al*. Precise radiochromic film dosimetry using a flat-bed document scanner. Med Phys 2005;32:2245-53.
28. Kong M, Holloway L. An investigation of central axis depth dose distribution perturbation due to an air gap between patient and bolus for electron beams. Australas Phys Eng Sci Med 2007;30:111-9.
29. Sharma SC, Johnson MW. Surface dose perturbation due to air gap between patient and bolus for electron beams. Med Phys 1993;20 (2 Pt 1):377-8.
30. Klein EE, Kashani R. Electron-beam therapy dosimetry, treatment planning, and techniques. In: Halperin EC, Brady LW, Wazer DE, Perez CA, editors. Perez and Brady's Principles & Practice of Radiation Oncology. 6th ed. Philadelphia: Lippincott Williams & Wilkins; 2013. p. 178-202.
31. Low DA, Starkschall G, Bujnowski SW, Wang LL, Hogstrom KR. Electron bolus design for radiotherapy treatment planning: Bolus design algorithms. Med Phys 1992;19:115-24.
32. Højris I, Overgaard M, Christensen JJ, Overgaard J. Morbidity and mortality of ischaemic heart disease in high-risk breast-cancer patients after adjuvant postmastectomy systemic treatment with or without radiotherapy: Analysis of DBCG 82b and 82c randomised trials. Radiotherapy Committee of the Danish Breast Cancer Cooperative Group. Lancet 1999;354:1425-30.
33. Archambeau JO, Forell B, Doria R, Findley DO, Jurisch R, Jackson R. Use of variable thickness bolus to control electron beam penetration in chest wall irradiation. Int J Radiat Oncol Biol Phys 1981;7:835-42.